Cement and Concrete Research 42 (2012) 186–193

Contents lists available at SciVerse ScienceDirect

Cement and Concrete Research

journal homepage: http://ees.elsevier.com/CEMCON/default.asp

Microstructure of cement paste subject to early carbonation curing

Vahid Rostami [a], Yixin Shao [a,*], Andrew J. Boyd [a], Zhen He [b]

[a] Department of Civil Engineering and Applied Mechanics, McGill University, 817 Sherbrooke Street West, Montreal, Quebec, Canada H3A 2K6
[b] School of Water Resources and Hydropower Engineering Science, Wuhan University, Wuhan, China

ARTICLE INFO

Article history:
Received 16 July 2011
Accepted 21 September 2011

Keywords:
Carbonation (C)
Microstructure (B)
Curing (A)
Compressive strength (C)
Calcium–Silicate–Hydrate (B)

ABSTRACT

Microstructure of Ordinary Portland Cement paste subjected to early age carbonation curing was studied to examine the effect of early carbonation on performance of paste at different ages. The study was intended to understand the mechanism of concrete carbonation at early age through the microstructure development of its cement paste. Early carbonation was carried out after 18-hour initial controlled air curing. The microstructure characterized by XRD, TGA, ^{29}Si NMR and SEM was correlated to strength gain, CO_2 uptake and pH change. It was found that early carbonation could accelerate early strength while allowing subsequent hydration. The short term carbonation created a microstructure with more strength-contributing solids than conventional hydration. Calcium hydroxide was converted to calcium carbonates, and calcium–silicate–hydrate became intermingled with carbonates, generating an amorphous calcium–silicate–hydrocarbonate binding phase. Carbonation modified C–S–H retained its original gel structure. The re-hydration procedure applied after carbonation was essential in increasing late strength and durability.

1. Introduction

Concrete is well known to be reactive with carbon dioxide. When this carbonation reaction occurs in freshly cast cement and concrete, the process has been shown to offer improved mechanical [1–3] and durability [4] properties. It is believed that carbonation of fresh dicalcium silicate (C_2S) and triclacium silicate (C_3S) pastes is an accelerated curing process, with the governing reactions shown by Eqs. (1)–(2). The carbonation reaction products are a hybrid of calcium–silicate–hydrate (C–S–H) and calcium carbonate ($CaCO_3$). High early strength can be obtained within a few minutes to a few hours [1, 3].

$$C_3S + (3-x)CO_2 + yH_2O \rightarrow C_xSH_y + (3-x)CaCO_3 \quad (1)$$

$$C_2S + (2-x)CO_2 + yH_2O \rightarrow C_xSH_y + (2-x)CaCO_3 \quad (2)$$

The carbonation reaction could also occur in mature concrete during service (Eqs. (3)–(4)). Atmospheric carbon dioxide reacts with hydration products, such as calcium hydroxide (CH) and calcium silicate hydrate (C–S–H), forming $CaCO_3$ and silica gel:

$$Ca(OH)_2 + CO_2 \rightarrow CaCO_3 + H_2O \quad (3)$$

$$C\text{–}S\text{–}H + 2CO_2 \rightarrow SiO_2 + 2CaCO_3 + H_2O \quad (4)$$

Extensive investigations into weathering carbonation of hydration products have suggested that the reactions of CH and C–S–H with carbon dioxide are dominant in atmospheric carbonation [5, 6]. It was found that atmospheric carbonation of well hydrated tricalcium silicate for over two years has led to complete carbonation and decalcification of C–S–H and formation of silica gel and partial carbonation of CH [5]. A 100-day carbonation of 28-day hydrated Ordinary Portland Cement (OPC) using natural weathering carbonation lowered the Ca/Si of the C–S–H. Carbonation of the same duration performed on the same hydrated OPC paste using 10% and 100% pure CO_2, decalcified the C–S–H completely [6].

Carbonation of mature concrete exposed to atmospheric carbon dioxide is not a desired chemical reaction. It generates carbonation shrinkage and reduces the pH value of the pore solution in concrete, leading to restrained concrete cracking and carbonation-induced steel corrosion [7]. However carbonation at early ages can be beneficial, acting as an accelerated curing technique [1, 3] that can considerably improve the durability performance of concrete due to the elimination of CH [4]. A recent study showed that two-hour carbonation curing of concrete after 18 h of pre-setting can effectively replace steam curing for precast concrete production [8]. Concrete carbonated on this manner has comparable strength to steam-cured concrete and exhibits an enhanced resistance to permeation, sulfate attack, and freeze–thaw damage. Subsequent hydration after early carbonation contributes significantly to late strength gain and maintains concrete alkalinity above the threshold value. The early carbonation of precast concrete could reduce the carbonation shrinkage of assembled concrete structures in service [9]. In addition to the technical advantages, early carbonation curing is a CO_2 sequestration process that

---

* Corresponding author. Tel.: +1 514 398 6674; fax: +1 514 398 7361.
E-mail address: yixin.shao@mcgill.ca (Y. Shao).

0008-8846/$ – see front matter © 2011 Elsevier Ltd. All rights reserved.
doi:10.1016/j.cemconres.2011.09.010

is capable of utilizing carbon dioxide recovered from cement kiln flue gas, allowing for carbon recycling within the cement and concrete industry [10].

This paper presents a study on the microstructure development of a cement paste subject to two-hour carbonation curing after an initial setting of 18 h in an attempt to understand the performance of concrete subject to a similar early carbonation process. While research on the carbonation of fresh cement paste or mature concrete are extensive, work on early carbonation of cement paste after initial setting but within 24 h followed by a subsequent hydration cycle is scarce. Nevertheless, this process window is more feasible for large scale production than immediate carbonation of fresh products. Carbonated cement pastes are compared with traditionally hydrated references by strength gain, carbon uptake and pH value at early and late ages. The progressive microstructure changes are characterized by X-Ray diffraction (XRD) analysis, thermogravimetry analysis (TGA), ^{29}Si nuclear magnetic resonance (NMR) spectroscopy and Scanning Electron Microscopy (SEM).

2. Experimental procedure

CSA (Canadian Standard Association) Type GU Ordinary Portland Cement (Holcim OPC) was used in preparing cement paste samples. Its chemical composition, as determined by XRF, is presented in Table 1. Cement paste samples were selected to eliminate the influence of aggregates on the microstructural analysis. To study the effect of early carbonation on concrete through microstructure change of cement paste, cement paste samples were prepared with same water to cement ratio of 0.36 as used in concrete [8]. This w/c ratio was chosen to represent a group of precast concretes such as masonry blocks, sewage pipes and hollow core slabs. At this w/c, early carbonation of concrete requires an initial curing to reduce free water and allow carbon dioxide diffusion [8]. To assure that the final water content in the cement paste remained the same as in concrete after initial curing, a thickness of 6 mm was selected through trial tests. The initial curing was carried out in an environmental chamber at 25 °C and 60% relative humidity (RH) for 18 h. The duration was chosen to represent overnight initial curing for a daily work shift. Strips of cement paste 200 mm long, 14 mm high and 6 mm thick were cast in a mold and then cut into samples of 14 mm × 14 mm × 6 mm while they were still in plastic state. These test specimens were then cured in an environmental chamber for 18 h. The final percent water content in the paste after initial curing was kept the same as in concrete. Therefore, the paste samples so prepared represented the paste in concrete reported in a prior study [8].

Seven batches, shown in Table 2, were cast with the same w/c but treated with different curing regimes. The sealed hydrated reference (B2 and B9) were kept in a sealed condition up to tests at 20 h and 28 days without water loss. B1 and B8 were also hydration references that were initially cured in an environmental chamber at a RH of 60% at 25 °C for 20 h. B1 specimens were tested right after this 20 h period while B8 specimens were sealed for an additional 27 days of hydration after the 20 h in the environmental chamber. B3, B10 and B11 were initially air cured in the same environmental chamber for 18 h and then carbonated together for 2 h in a CO_2 chamber. After 18 h of initial curing and 2 h of carbonation, B3 specimens were tested immediately for 20-h strength and B10 specimens were sealed for an additional 27 days of hydration before being tested at 28 days. To examine the effect of water loss during initial air curing on subsequent hydration, B11 specimens were water sprayed right after carbonation curing to compensate for total water loss during air and carbonation curing periods and then sealed for subsequent hydration of 27 days.

Table 1
Chemical composition of the cement.

Constituent %									
CaO	SiO_2	Al_2O_3	Fe_2O_3	MgO	Na_2O	K_2O	SO_3	CO_2	LOI
63.1	19.8	4.9	2	2	0.85*	–	3.8	1.89	1.66

* Na_2O alkali equivalent including K_2O.

Table 2
Curing regimes.

Batch	ID	Initial curing	Subsequent curing	Test age
B1	20A	20 h air curing*	0	20 h
B2	20S	20 h sealed curing	0	20 h
B3	18A + 2C	18 h air curing* + 2 h carbonation	0	20 h
B8	20A	20 h air curing*	27 days in sealed bag	28 days
B9	20S	20 h sealed curing	27 days in sealed bag	28 days
B10	18A + 2C	18 h air curing* + 2 h carbonation	27 days in sealed bag	28 days
B11	18A + 2C + WS	18 h air curing* + 2 h carbonation + water spray	27 days in sealed bag	28 days

* Air curing in RH = 60%, T = 25 °C.

Fig. 1 shows the early carbonation curing setup. After air cured samples were placed in the chamber, carbon dioxide of 99.5% purity was injected to and kept at a constant pressure of 0.15 MPa so that CO_2 absorbed by the cement would be replenished. The chamber was then placed on an electronic balance and the mass of the entire system was recorded. The balance was zeroed before the gas was injected and the subsequent mass curve was used to quantify the percent carbon uptake by cement paste after correction for residual gas in the chamber [4]. A second method used to determine CO_2 uptake was the mass gain method that compares the sample mass before and after carbonation. The mass difference, together with the lost water due to exothermic reactions, represents carbon uptake. The lost water was condensed on the wall of chamber and collected by absorbent paper. The CO_2 uptake was calculated based on cement mass:

$$CO_2 \text{ uptake } (\%) = \frac{(\text{Mass}_{\text{aftercarbonation}} + \text{Water}_{\text{lost}}) - \text{Mass}_{\text{beforecarbonation}}}{\text{Mass}_{\text{cement}}} \quad (5)$$

Compressive strengths at 20 h and 28 days were tested using a compression area of 14 × 6 mm. Ten samples of each batch were tested at each specified age to produce a representative average. The fractured samples were collected for XRD, pH, TGA, NMR and SEM analysis. Samples were preserved in acetone to stop further hydration. The acetone was refreshed on each of three consecutive days to make sure all the free water was washed out of the samples. Before making powder samples for analysis, they were dried overnight at 60 °C.

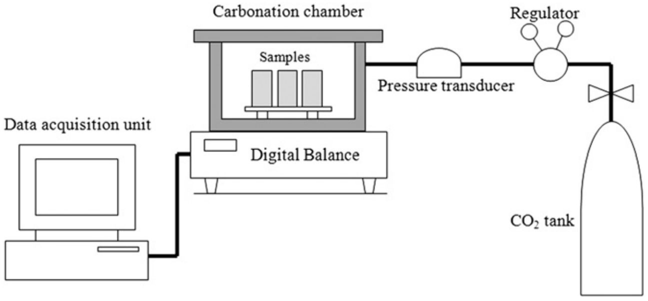

Fig. 1. Early carbonation curing set up.

The pH values of carbonated and hydrated samples were measured after compressive tests employing a simple ion extraction method [11]. Distilled water of 100 μl was dropped on an absorbent paper on the paste sample surface. After 15 min, which was determined to be sufficient to produce constant values, the pH of the solution extracted by the paper was measured using a pH meter (Extech PH110) with a flat sensor head of 9 mm diameter. Three samples in each batch were chosen for the measurements and the values were averaged.

Crystalline phases of carbonated and hydrated cement pastes were analyzed using a Phillips PW1710 Power Diffractometer (Cu Kα radiation, scan interval 15–55° 2θ, 0.02° and 0.5 s per step). For carbonated samples, powders were taken from both surface (outer 2 mm) and core (middle 2 mm) for comparison. The same powder sample of 100 mg used for XRD was also examined for thermogravimetry analysis. A thermal analyzer (NETZSCH, TG 449F3 Jupiter) with a resolution of 0.01 mg was employed to run TGA and obtain the mass loss of the samples in the range 25 °C to 950 °C at the heating rate of 10°/min.

To study the effect of the carbonation treatment on silicate structure of C–S–H, ^{29}Si NMR spectra were obtained at 59.5 MHz using an Agilent/Varian VNMRS-300 spectrometer. Samples of constant mass of 100 μg were collected from the 2 mm surface layer, packed in 7.5 mm zirconia rotors, and spun at 4000 Hz. A $\pi/2$ pulse of 5 μs was applied with a recycle delay of 5 s.

The fracture surfaces of the samples were also examined using a variable pressure (VP) SEM in SE mode to study the morphology of the paste in the near surface zone at different stages of carbonation.

3. Results

3.1. Early carbonation behavior after initial air curing

Table 3 summarizes the percent water content of batches after different initial curing treatments. The calculation was based on the initial mixing water, considering the water content as being 100% immediately after casting. Except for the sealed hydrated reference batches (B2 and B9), all other samples experienced water loss during the initial curing. The 18-hour air curing at 60% RH and 25 °C lowered the water content in the samples of batches B1, B3, B8, B10 and B11 down to about 60% of the initial mixing water. Air curing in a controlled environment is crucial to early carbonation curing. It removes part of the free water and allows a diffusion-controlled carbonation reaction. The subsequent 2-hour carbonation cycle led to further water loss in the carbonation batches B3, B10 and B11 due to exothermic reaction according to Eqs. (1)–(2). However, this loss was less than 4% of the initial water. Water loss could be detrimental for long term hydration. To restore initial water content in the carbonated batches, the water lost due to both air and carbonation curing was replaced by water spray in Batch 11. It was possible to replace all of the lost water to carbonated cement and reach the original water content of 100%. After the water spray, the B11 samples were sealed in plastic bags for subsequent hydration. The final water content of each batch is shown in Table 3.

The early carbonation behavior of the cement pastes was characterized by strength gain, CO_2 uptake and pH value. Results are summarized in Table 4. Comparison of carbonated cement paste (B3) with the hydration references (B1 and B2) revealed significantly accelerated early strength gain due to the 2-hour carbonation treatment. Although there was significant water loss in the carbonated cement paste, the 20-hour strength was still higher in the carbonated (B3) than in the hydrated reference without water loss (B2). It was noted that water loss in air curing made the reference B1 weaker than the B2 reference. Considerable strength gain was observed in carbonated cement paste at 28 days. The strength gain due to the hydration progress suggested that early carbonation did not hinder subsequent hydration. Carbonated cement paste (B10) exhibited higher strength than reference with the same water loss (B8) but lower strength than reference without water loss (B9). This indicates that early age water loss due to air curing had a negative effect on subsequent hydration. The water spray seemed to be a simple and effective method to solve the problem. The strength gain in carbonated cement paste after exposure to the water spray (B11) exhibited the highest strength at 28 days. It is likely that if water content can be replenished to its original level, early carbonation curing can be utilized to its best advantages. This finding suggests that in general a strong paste structure can be formed after a short carbonation period followed by conventional hydration.

The CO_2 uptake by cement pastes subjected to 2-hour carbonation is also summarized in Table 4. The uptakes by two methods are of close value and their average is in the range of 8% based on dry cement mass. Carbonation is also evidenced by the change in pH values. The air cured reference (B1) showed a slightly lower pH value at 20 h, compared to the sealed hydrated reference (B2), due to a lower degree of hydration. The 2-hour carbonation cycle reduced the pH about one unit in B3 at 20 h, due to partial consumption of the CH phase. The carbonated samples with and without water spray treatment (B11 and B10, respectively) manifested different pH values after 27 days of subsequent hydration. The carbonated paste with water spray (B11) became more alkaline with an increased pH value, while the pH of the carbonated paste without additional water (B10) did not change significantly after 27 days. Subsequent hydration appeared to be critical in this early carbonation curing process. If sufficient water is available after early carbonation, the performance of the carbonated cement can be comparable to the best reference. Although the total alkalinity of B11 was still slightly lower than that in the best reference samples (B9), carbonated cement can still maintain a sufficiently high pH to avoid depassivation of embedded reinforcing steel. It is indicative that early carbonation treatment could be considered applicable to precast reinforced concrete.

Table 3
Change of water content in paste samples with respect to mixing water.

Batch ID	Water content with respect to mixing water (%)				
	After mixing	After air curing	After carbonation	After water spray	Remaining water
B1	100	59.4	n/a	n/a	59.4
B2	100	n/a	n/a	n/a	100
B3	100	63.1	59.3	n/a	59.3
B8	100	60.4	n/a	n/a	60.4
B9	100	n/a	n/a	n/a	100
B10	100	62.8	59.1	n/a	59.1
B11	100	62.6	58.9	100	100

Table 4
Strength, pH and carbon uptake.

Batch ID	Strength (MPa)	CO_2 uptake (%)		pH
		Mass gain	Mass curve	
B1	31.0 ± 4.1	n/a	n/a	12.6 ± 0.1
B2	35.8 ± 2.6	n/a	n/a	13.0 ± 0.1
B3	50.0 ± 5.4	7.6	8.9	11.3 ± 0.2
B8	47.2 ± 5.3	n/a	n/a	12.9 ± 0.1
B9	97.2 ± 5.9	n/a	n/a	13.1 ± 0.2
B10	76.8 ± 6.4	7.6	8.9	11.8 ± 0.1
B11	123.7 ± 11.8	7.5	8.9	12.3 ± 0.1

3.2. Phase analysis

The XRD patterns of all batches are presented in Figs. 2 and 3. While Fig. 2 presents the XRD patterns in the 2-mm surface layer, Fig. 3 compares samples taken from the surface and the core. In Fig. 2, comparing B3 with B1 indicates that the CH proportion is significantly reduced at the surface after carbonation, whereas at the same time, calcium carbonates are generated. The presence of residual CH even in the highly carbonated zone might be due to isolation of the CH crystals by calcite formation on its surface, a phenomenon also observed by other researchers [12]. A noticeable reduction in the peak intensity of B3 at 32.3 °C corresponding to two over lapping peaks of C_2S and C_3S was detectable. It might suggest that C_2S or C_3S was partially carbonated.

Comparing B3 and B11 in Fig. 2 suggests that further hydration occurred in the carbonated zone of water-sprayed cement, since the CH peaks grow stronger and C_3S and C_2S are noticeably diminished. However, there is no strong evidence to show CH growth in B10, indicating a weak subsequent hydration due to lack of water.

Fig. 3 compares the degree of carbonation at the surface and in the core. The core samples for XRD were taken from 2 to 4 mm depth. At early age, no significant carbonation occurs in the core of the carbonated cement if the XRD trace of the B3 core (Fig. 3) is compared with that of the reference B1 (Fig. 2). Comparison of the B3 and B11 cores suggests subsequent hydration progress, as CH peaks appear to be stronger and calcium silicate peaks weaker after 28 days in a sealed condition.

3.3. TGA/DTG results

Fig. 4 compares enlarged TGA and DTG curves of hydrated (B9) and carbonated (B11) batches. For the carbonated batches, powder samples were taken from the surface of carbonated cement pastes. A steeper mass loss between 105 and 150 °C is evident in the B9 TGA curve indicates CSH dehydration [13]. The TGA curve corresponding to the carbonated sample exhibits a low rate of mass loss due to CH decomposition at 420–460 °C, while the reference sample shows a higher rate of mass loss in the same range. The mass loss after 540 °C is attributed to decarbonation. Thus, the steeper curves in the carbonated cements clearly indicate the onset and the rate of loss of bonded CO_2.

DTG curves of all batches are compared in Fig. 5. Mass loss between 105 and 420 °C represents the loss of combined water due to dehydration of calcium silicate hydrate, aluminate hydrate and ferroaluminate hydrate [13–15]. The loss between 420 and 540 °C corresponds to the dehydration of calcium hydroxide [13, 14]. Decarbonation of well-crystalline calcium carbonate occurs at temperatures between 720 and 950 °C [16]. The loss between 540 and 720 °C is likely associated with poorly-crystalline calcium carbonate [17, 18].

Comparing the curves of B1 with B3, it can be seen that dehydration of CH at 450 °C is less intensive in carbonated cement pastes, indicating the CH consumption due to carbonation. The peak intensities around 750 °C in the reference hydration cement pastes are weak and represent initial carbon content in as-received cement or due to atmospheric carbonation. Contrarily, the peaks around 800 °C in the carbonated are strong. These peaks confirm the formation of strong crystalline calcium carbonates.

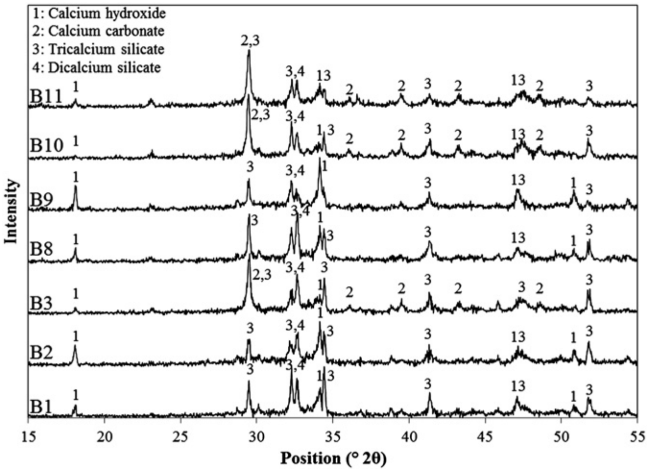

Fig. 2. XRD patterns of cement pastes from surface of samples.

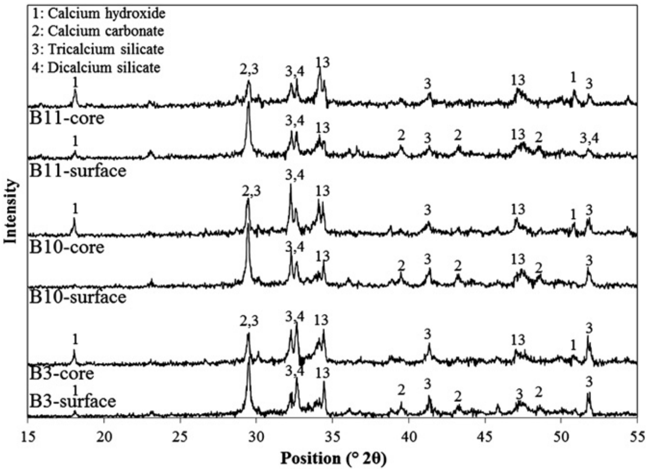

Fig. 3. Comparison of XRD patterns on surface and at core of carbonated pastes.

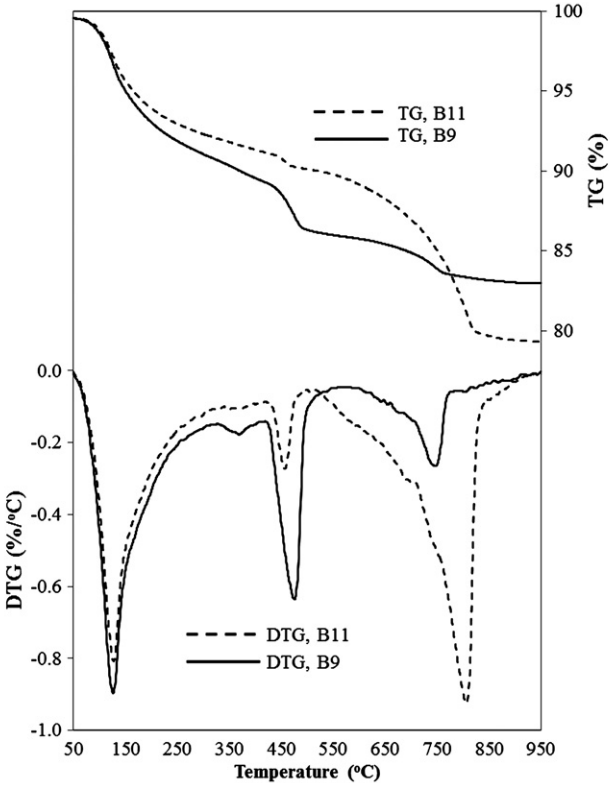

Fig. 4. Typical TGA and DTG curves of paste samples in batches B9 and B11.

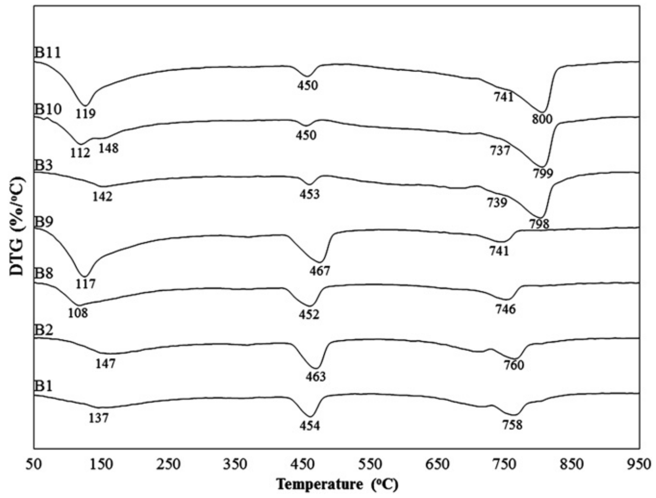

Fig. 5. Comparison of DTG curves of paste samples at early (20 h) and late (28 days) age.

The weight losses corresponding to all endothermic events between 105 and 540 °C are summarized in Fig. 6. Water losses between 105 and 540 °C represent decomposition of hydration products. Temperature of 105 to 200 °C induce decomposition of C–S–H gel, ettringite and gypsum, 200 to 420 °C — C_3A and C_4AF hydration products [13, 14], 420 to 540 °C — calcium hydroxide. However, if water is more firmly bonded in the C–S–H, it is still likely that some C–S–H dehydration will occur up to 300 °C [19].

By comparing early age batches B1 and B3, it can be seen that the water loss corresponding to temperature ranges below 420 °C shows no significant difference, suggesting that the short carbonation period does not alter the structure of the binding phases with the exception that CH is noticeably reduced. Examining carbonated pastes (B3 and B11) by comparing water losses at different temperature ranges reveals that the water losses between 105–200 °C and 420–540 °C are noticeably increased. This implies a significant increase in hydration after carbonation, which is in agreement with strength test results. It is interesting to compare B11 with B9. The carbonated cement paste exhibits less hydration products than the hydration reference owing to significantly reduced CH, as well as C_3A and C_4AF hydration products. The content of C–S–H gel nevertheless seems to be comparable. Hydration degree is low in B8 and B10, in which water loss due to initial air curing is the direct cause.

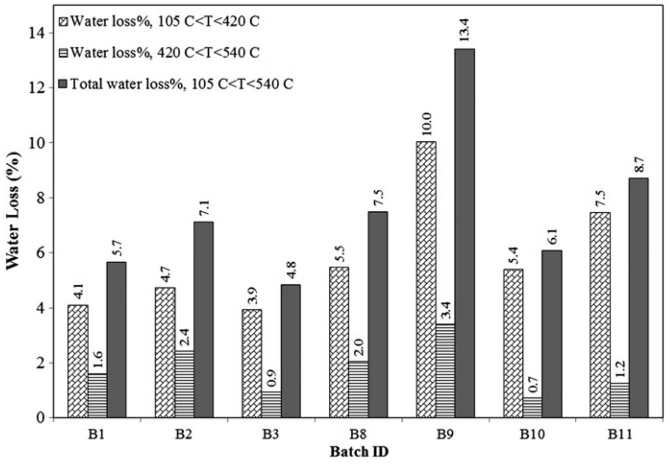

Fig. 6. Water loss of pastes due to dehydration.

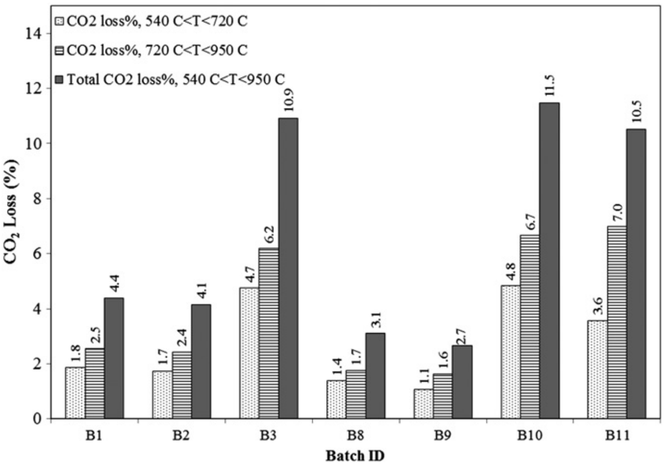

Fig. 7. CO_2 loss of pastes due to decarbonation.

The CO_2 content of the samples, determined by weight loss above 540 °C, is presented in Fig. 7. It is evident that the carbonated batches contain much higher carbon contents compared to the reference samples. The CO_2 loss in the reference samples were most likely due to carbonates in the as-received cement and atmospheric carbonation, since no strict measures were taken to prevent air carbonation during mixing and air curing. Higher CO_2 content in the reference paste compared to that of as-received cement given in Table 1 could verify occurrence of air carbonation during making samples.

Two different ranges of CO_2 loss were distinguished using DTG peaks, being 540–720 °C and 720–950 °C. The carbonates decomposing at a higher temperature range could suggest a highly crystalline phase. It is interesting to study the distribution of the bonded CO_2 between the two temperature ranges; comparing the carbon loss of B1 and B3, it can be seen that at lower temperatures, less CO_2 was released compared to that of higher temperature; it can be implied that during the short term carbonation, CO_2 was primarily converted to a highly crystalline form, from carbonation of calcium silicates and CH. In addition, the carbonates produced from carbonation of C–S–H, represented by a CO_2 loss between 540 and 720 °C [12, 16, 17], showed the least thermal stability, suggesting poorly crystalline calcium carbonate.

The total mass losses of the samples are presented in Table 5. Carbonated samples exhibited higher mass losses compared to hydrated references at both early and late ages. Comparing the value for hydrated reference sample B9 and B11 suggests that carbonated cement contains more hydration and carbonation products. This explains why carbonated cement paste with water spray (B11) is stronger than the hydrated reference without water loss (B9).

Using the CO_2 loss data obtained from the TGA test, CH and $CaCO_3$ were quantified for all of the batches and the corresponding contents are presented in Table 6. The amount of calcium carbonates could be generated due to carbonation of the CH produced during the 18-hour air curing (B1), which was estimated using stoichiometric calculation to be $(100/74 \times (6.5–3.8)\% = 3.6\%)$, according to Eq. (3). The numbers 100 and 74 are the molar masses of calcium carbonates and CH, respectively. Taking into account the initial calcium carbonates present in the non-hydrated samples (10.0%), the total calcium carbonate content that could be expected assuming only CH carbonation would be 13.6% $(13.6\% = 3.6 + 10.0)$. However, this calcium carbonate content

Table 5
Total mass loss of cement paste in TGA test.

Batch ID	B1	B2	B3	B8	B9	B10	B11
Total mass loss (%)	10.1	11.3	15.8	10.6	16.1	17.6	19.2

Table 6
Calcium hydroxide and calcium carbonate content in paste samples.

	Phase content (%)						
	B1	B2	B3	B8	B9	B10	B11
Calcium hydroxide	6.5	9.9	3.8	8.4	13.9	2.9	5.1
Calcium carbonate	10.0	9.4	24.8	7.0	6.1	26.1	23.9

is much smaller than the amount measured in B3 (24.8%), which supports the hypothesis that carbonation of phases other than CH, such as calcium silicates and C–S–H, had occurred.

Comparing the amount of carbonation-induced calcium carbonates decomposed after 720 °C with those produced due to CH carbonation in B3 can illustrate whether carbonation of phases other than CH also generated high thermally stable carbonates. The former was calculated to be 3.6%, while the latter can be estimated using Fig. 7 and Eq. (3) to be 8.2% ($(100/44)\times(6.2\text{–}2.5)\% = 8.2\%$), where the values 100 and 44 are the molar masses of $CaCO_3$ and CO_2, respectively. This observation suggests that more than half of the well crystalline calcium carbonates were formed due to carbonation of phases other than CH, including C–S–H and calcium silicates.

It is also worth comparing the CH contents in B3 and B11; the extent of subsequent hydration can be estimated comparing CH content in these two batches. The CH content was increased in the water sprayed batch (B11), suggesting hydration of unreacted calcium silicates in the carbonated zone occurred after the early age carbonation, which is in agreement with XRD observation. However, comparing XRD results corresponding surface and the core of the samples clearly indicated that more hydration occurred in the non-carbonated core of the paste after the first 24 h.

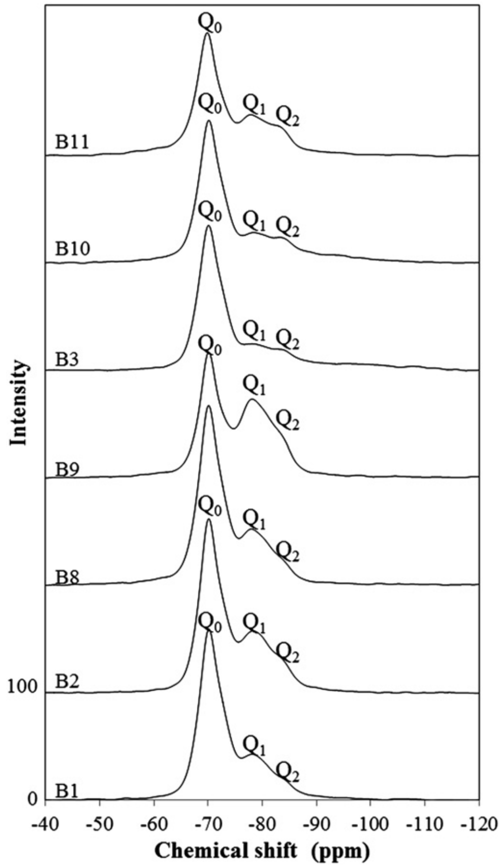

Fig. 8. ^{29}Si NMR spectra of carbonated and reference samples (peaks are approximately at $Q_0 = -70$ ppm, $Q_1 = -79$ ppm and $Q_2 = -83$ ppm).

Table 7
Q numbers obtained from ^{29}Si NMR.

Batch ID	Q_0	Q_1	Q_2	Q1/Q2
B1	157	41	24	1.71
B2	161	57	39	1.46
B3	132	24	20	1.20
B8	159	50	34	1.47
B9	112	72	51	1.41
B10	130	28	24	1.17
B11	113	37	29	1.28

3.4. NMR results

The ^{29}Si NMR spectra of all batches are plotted in Fig. 8. The peaks of chemical shift are designated as Q_0, Q_1 and Q_2, the values of which are summarized in Table 7. Q_0 represents the percentage of unreacted calcium silicates, while Q_1 and Q_2 reflect the percentage of dimer and linear chain bonds in C–S–H, respectively. As hydration progresses, Q_0 decreases while Q_1 and Q_2 increase, as can be seen in the reference samples B2 and B9. Comparing the results from B1 and B3 reveals that the Q_1/Q_2 ratio decreased due to carbonation, suggesting carbonation had enhanced degree of polymerization of C–S–H in comparison to reference. No Q_3 and Q_4 were observed in this short term carbonation indicating no silica gel was generated from early carbonation [17]. Since carbonated cement paste had shown an early strength that was significantly higher than the hydration reference, it is implicated that C–S–H structure developed due to carbonation is stronger owing to the silica dimers and liner chains integrated with calcium carbonates. This phenomenon was not observed in previous studies on carbonation of hydration products in a mature concrete, where high degrees of polymerization had been reported [5, 17].

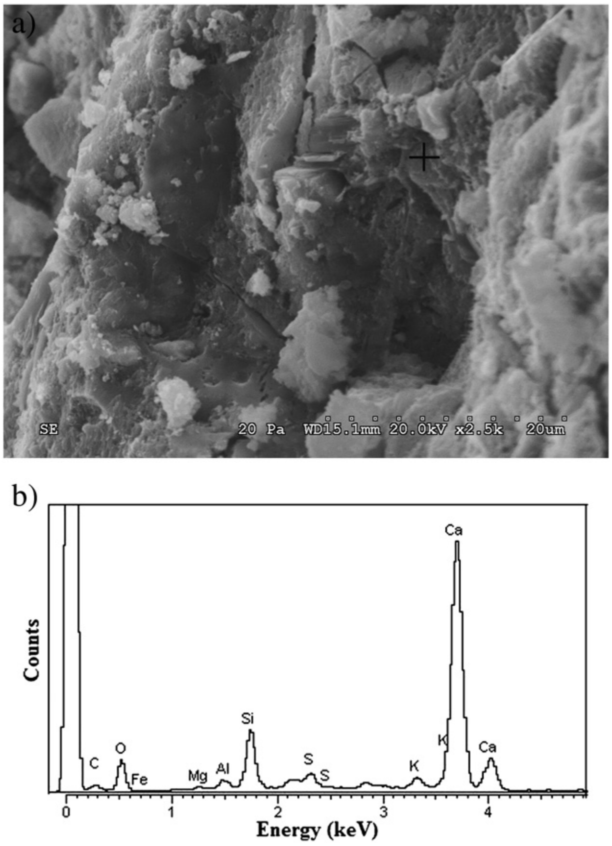

Fig. 9. Air cured OPC paste at 20 h (B1): a) SEM photomicrograph. b) EDS analysis.

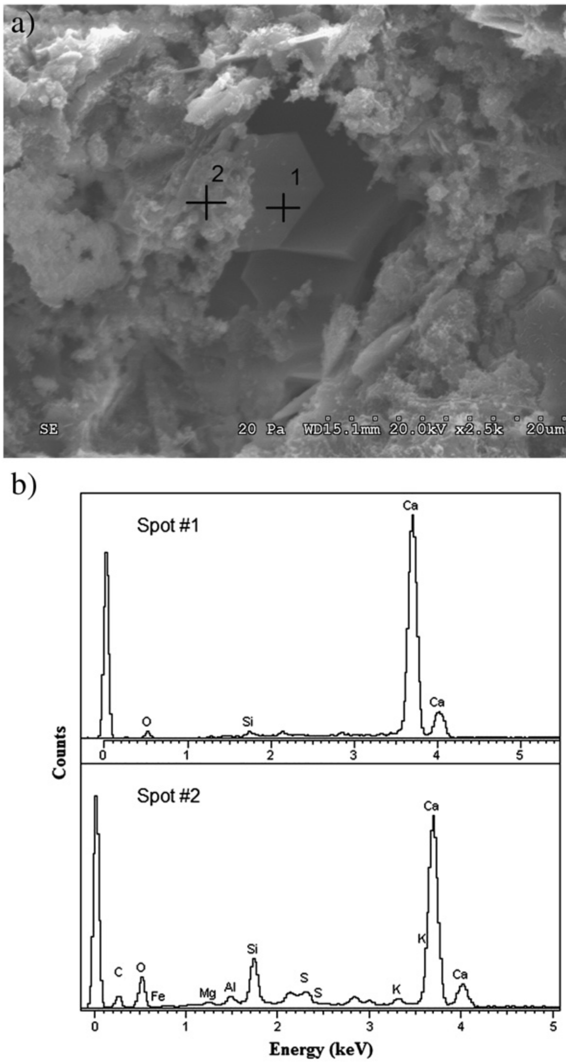

Fig. 10. Sealed cured OPC paste at 28 days (B9): a) SEM photomicrograph. b) EDS analysis.

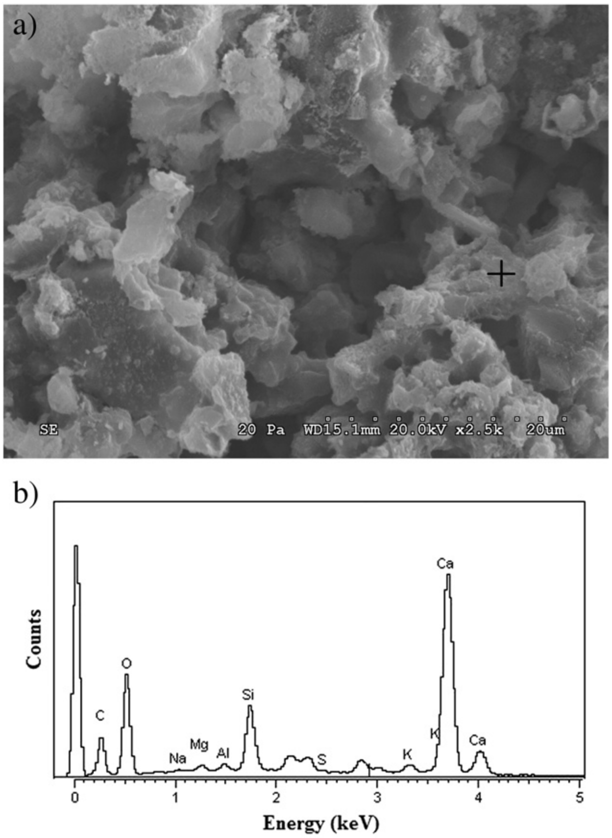

Fig. 11. Carbonated OPC paste at 20 h (B3): a) SEM photomicrograph. b) EDS analysis.

3.5. SEM

Figs. 9–12 present typical SEM photomicrographs of OPC pastes taken in secondary electron (SE) mode for the different curing procedures. Fig. 9 shows the paste sample before carbonation (B1). EDS analysis suggests strong peaks of Ca, Si and O. The high content of the designated elements indicates the presence of calcium silicate hydrates generated in vicinity of calcium silicates after 18 h of controlled air curing. Fig. 10 presents the microstructure of the reference cement paste (B9) after 28 days of hydration without water loss. It is composed of typical amorphous C–S–H and crystalline CH.

Fig. 11 shows the typical features of a carbonated paste (B3). Generally, the carbonated paste has finer texture compared to the hydration reference (B1 in Fig. 9). While the corresponding XRD pattern suggests formation of carbon products, the SEM picture does not provide any evidence of the crystalline form of carbonates. However, a monolithic amorphous C–S–H containing relatively high carbon content can be distinguished based on the Energy Dispersive Spectroscopy (EDS) spot analysis (Fig. 11b). This result suggests that the C–S–H phase is modified by carbonates, which is in agreement with the thermogravimetric results. In addition, pure calcium carbonate is not detected; instead it is always intermingled with C–S–H gel.

Fig. 12 shows the carbonated sample after 27 days of subsequent hydration (B11). The EDS analysis of the spots shown reveals strong intensities of Ca, Si, O and C, suggesting the existence of a hybrid of hydrates and carbonates. Comparison of relative intensities of carbon and oxygen in Fig. 11 with those in Fig. 12 suggests that O/C is noticeably greater in the B11 sample. This can serve as supporting evidence of subsequent hydration in the carbonated zone, as was revealed from XRD, NMR and TGA analysis.

4. Discussion

Early carbonation curing is different from weathering carbonation. Early carbonation curing is performed after 18 h of hydration and consists of only 2 h of exposure to CO_2. Therefore, the degree of carbonation is not high and subsequent hydration can still proceed. In contrast, weathering carbonation of mature concrete occurs after completion of hydration and is detrimental to structure of hydrated cement paste. Decalcification of C–S–H and formation of silica gel are the direct consequence [5]. However, the short-term early age carbonation investigated in this research did not lead to silica gel formation and no significant reduction in pH value. Instead the carbonated cement paste at early age was enhanced by further hydration.

According to the NMR results obtained in this research, carbonated C–S–H did not undergo further polymerization after the short term carbonation. Early carbonation decreases Q_1/Q_2 ratio, suggesting carbonation modified C–S–H is Si-rich but its binding capacity by Ca–O structure is maintained. The formation of calcium carbonates is evidenced by carbon uptake, accelerated strength gain, calcite peak in XRD and endothermic peaks by DTG. However there are no clear crystals of micron size under SEM. Although existence of carbon is also evident by EDS analysis, the binding phase is typical of amorphous. Because of carbonation, calcium content in C–S–H is reduced, leading to a change in silica structure in combination of silica dimers and linear chains with no crosslinking. Therefore calcium carbonates may coexist in nano crystal size within C–S–H gel of the same order of magnitude. This is a beneficial characteristic for early carbonation:

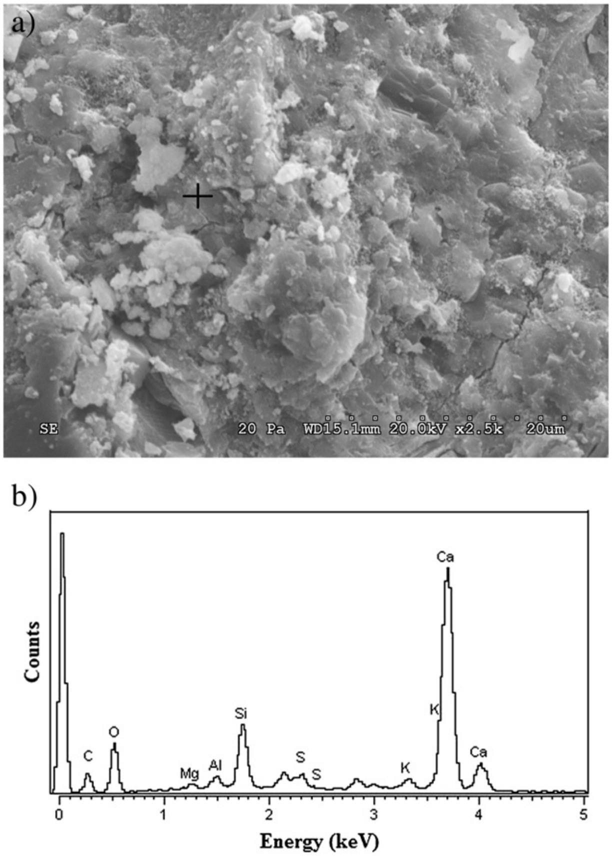

Fig. 12. Carbonated OPC paste at 28 days (B11): a) SEM photomicrograph. b) EDS analysis.

early strength of concrete is accelerated, surface layer of concrete is densified and chemically unstable calcium hydroxide is reduced. At the same time C–S–H gel can retain amorphous nature and comparable pH value for steel protection. Concrete so produced will also show its capacity for carbon sequestration and will help utilize the flue gas CO_2 collected from cement production in a beneficial manner.

5. Conclusions

Early carbonation of cement paste after 18 h of controlled air curing has led to noticeable early strength gain which is likely attributed to the formation of an amorphous calcium silicate hydrocarbonate. The sum of hydration and carbonation solid products is much higher in carbonated cements than in hydrated references. Calcium hydroxide and calcium silicates are the first compounds to be carbonated, followed by C–S–H. Two-hour carbonation enables a carbon uptake of 8% in terms of cement mass, which corresponds to a degree of carbonation of 16%. At this reaction level, the pH of the cement paste is reduced by one unit immediately after carbonation but can be increased through subsequent rehydration to a value comparable to the hydration reference. Therefore, the early carbonation process appears to be applicable to accelerated curing of reinforced precast concretes. Although carbonated cement can maintain a pH value above the corrosion threshold, its calcium hydroxide content is much reduced. Early carbonation is therefore expected to significantly improve concrete durability.

Controlled air curing is necessary to allow carbon dioxide to diffuse into concrete. This process, however, evaporates free water, making concrete weaker after subsequent hydration. Adding lost water through a surface spray to the carbonated samples immediately after the carbonation cycle is critical toward long-term strength and durability. With sufficient water, subsequent hydration can take place after the carbonation cycle and 28-day strengths of carbonated cement can exceed that of best reference.

Early carbonation is different from weathering carbonation. The subsequent rehydration after early carbonation can compensate for water loss and pH reduction and is capable of producing concrete stronger and more resistant to permeation due to the formation of a greater proportion of solids. Early carbonation does not hinder subsequent hydration. If applied properly, early carbonation can result in both technical and environmental benefits.

References

[1] J.F. Young, R.L. Berger, J. Breese, Accelerated curing of compacted calcium silicate mortars on exposure to CO_2, J. Am. Ceram. Soc. 57 (1974) 394–397.
[2] R.L. Berger, J.F. Young, K. Leung, Acceleration of hydration of calcium silicates by carbon-dioxide treatment, Nat. Phys. Sci. 240 (1972) 16–18.
[3] C.J. Goodbrake, J.F. Young, R.L. Berger, Reaction of beta-dicalcium silicate and tricalcium silicate with carbon dioxide and water vapor, J. Am. Ceram. Soc. 62 (1979) 168–171.
[4] V. Rostami, Y. Shao, A.J. Boyd, Durability of concrete pipes subjected to combined steam and carbonation curing, Constr. Build. Mater. 25 (2011) 3345–3355.
[5] P.A. Slegers, P.G. Rouxhet, Carbonation of the hydration products of tricalcium silicate, Cem. Concr. Res. 6 (1976) 381–388.
[6] M. Castellote, L. Fernandez, C. Andrade, C. Alonso, Chemical changes and phase analysis of OPC pastes carbonated at different CO_2 concentrations, Mater. Struct. 42 (2009) 515–525.
[7] M.G. Richardson, Carbonation of Reinforced Concrete: Its Causes and Management, CITIS Ltd, Ireland, 1988.
[8] V. Rostami, Y. Shao, A.J. Boyd, Carbonation curing versus steam curing for precast concrete production submitted to, ASCE Journal of Materials in Civil Engineering, 2011.
[9] H.T. Toennies, Artificial carbonation of concrete masonry units, J. Am. Concr. I 56 (1960) 737–756.
[10] Y. Shao, M.S. Mirza, CO_2 sequestration using calcium–silicate concrete, Can. J. Civ. Eng. 33 (2006) 776–784.
[11] M. Heng, K. Murata, Aging of concrete buildings and determining the pH value on the surface of concrete by using a handy semi-conductive pH-meter, Anal. Sci. 20 (2004) 1087–1090.
[12] G. Villain, G. Platret, Two experimental methods to determine carbonation profiles in concrete, ACI Mater. J. 103 (2006) 265–271.
[13] V.S. Ramachandran, J.J. Beaudoin, Handbook of Analytical Techniques in Concrete Science and Technology, William Andrew Publishing/Noyes, 2001.
[14] W. Sha, E.A. O'Neill, Z. Guo, Differential scanning calorimetry study of ordinary Portland cement, Cem. Concr. Res. 29 (1999) 1487–1489.
[15] R.L. Sharma, S.P. Pandey, Influence of mineral additives on the hydration characteristics of ordinary Portland cement, Cem. Concr. Res. 29 (1999) 1525–1529.
[16] N.R. Short, P. Purnell, C.L. Page, Preliminary investigations into the supercritical carbonation of cement pastes, J. Mater. Sci. 36 (2001) 35–41.
[17] Z. Sauman, Carbonization of porous concrete and its main binding components, Cem. Concr. Res. 1 (1971) 645–662.
[18] S. Goto, K. Suenaga, T. Kado, M. Fukuhara, Calcium silicate carbonation products, J. Am. Ceram. Soc. 78 (1995) 2867–2872.
[19] V.S. Ramachandran, Kinetics of hydration of tricalcium silicate in presence of calcium chloride by thermal methods, Thermochim. Acta 2 (1971) 41–55.